A Planimetrically Accurate SPOT Image Mosaic of Buton Island, Sulawesi, Indonesia*

Khalid A. Soofi and *Roger S. U. Smith*
Exploration Research and Services Division, Conoco Inc., Ponca City, OK 74603
Robert Siregar
Conoco Indonesia Inc., P. O. Box 1367, Jakarta, Indonesia 10013

ABSTRACT: A new map of Buton Island has planimetric sea-level accuracy of about 50 metres. This map is based on a series of panchromatic images from the French SPOT satellite and Doppler ground control. A comparison of the coastline positions shows discrepancies as large as two kilometres between the best existing maps and this new SPOT map. This new map has proven very useful both for planning seismic and other logistics operations as well as for field use. The methods described herein may prove useful in other frontier areas of exploration.

Most of Buton Island is covered by three nominal SPOT scenes. However, during a year's time, no cloud-free scenes of Buton were acquired by SPOT. Conoco acquired eight SPOT scenes with complementary cloud cover. Each scene was geometrically corrected and then mosaicked to generate a final SPOT image mosaic of Buton that was nearly free of clouds. Two different digital methods were chosen to combine images. One method consisted of cutting and pasting cloud-free images while another method compared data on a pixel by pixel basis and attempted to choose the cloud free pixel.

INTRODUCTION

A NEW MAP OF Buton Island has a planimetric sea-level accuracy of about 50 metres. This map is based on a series of panchromatic images from the French SPOT satellite and ground control. A comparison of the coastline position shows discrepancies as large as two kilometres between the best existing maps and this new SPOT map. This new map has proven very useful both for planning seismic and other logistic operations as well as for field use. The methods described herein may prove useful in other frontier areas of exploration. Buton Island lies in the Banda Sea off the southeast arm of Sulawesi, about 1,750 kilometres east of Jakarta.

Over the past three years, Conoco had acquired Landsat and side-looking airborne radar (SLAR) images of Buton Island for geologic interpretation. Even though these images proved very useful for both geomorphic and geological interpretation, they could not be used as base maps because they lacked geometric fidelity. Landsat MSS images with a nominal pixel size of 79 metres are extremely difficult to correct to an accuracy better than 400 metres. Radar images are even more difficult to correct because of errors in aircraft navigation and their related effects on the image. Panchromatic SPOT images with a nominal resolution of 10 metres were therefore deemed the most cost-effective way of producing accurate base maps.

Most of Buton Island is covered by three nominal SPOT scenes. However, during a year's time, no cloud-free scenes of Buton were acquired by SPOT. Conoco acquired eight SPOT scenes with complementary cloud cover. Each scene was geometrically corrected and then mosaicked to generate a final SPOT image mosaic of Buton that was nearly free of clouds. Image processing was done digitally using a VAX 8650 computer and Conoco's implementation of Jet Propulsion Lab's (JPL) VICAR image processing software. Two different methods were chosen to combine images. One method consisted of cutting and pasting cloud-free images while another method compared data on a pixel by pixel basis and attempted to choose the cloud free pixel.

*Presented at the Eighth Thematic Conference on Geologic Remote Sensing, Denver, Colorado, 29 April - 2 May 1991.

INPUT DATA

In March of 1989 we examined all the available SPOT images of Buton Island, 273 in all, to find those images with the least cloud cover. Because none of the 273 available images was free of clouds, we decided that a series of SPOT images should be digitally combined to minimize the cloud cover in the final Buton mosaic. After much deliberation, Conoco acquired eight panchromatic SPOT images with complementary cloud cover. Table 1 lists the vital information for these images.

Scenes B3 and C2 had the best sun angles. Both the viewing geometry and solar illumination geometry of SPOT for scenes A1 and A2 were very similar. Because their radiometric character was very similar as well, they provided an ideal case for applying an algorithm devised to remove clouds. Parts of each of the eight images were then used in the final mosaic.

GROUND SURVEY

Conoco Indonesia Inc. contracted P.T. Alico to carry out a geodetic Doppler survey of Buton Island to determine the coordinates of 14 stations. P.T. Alico used Magnavox MX1502 satellite positioning receivers to establish station locations within five metres RMS, which is more than adequate for the correction of SPOT images. P. T. Alico conducted the survey between 29 July and 25 September 1988. Bakosurtanal station D-487 on the northern end of Muna Island was reoccupied using the point method and served as the master station. All other stations were translocated to the D-487 reference. These methods are discussed below.

The point method is the simplest method in satellite surveying, and it depends entirely on the assumption that geometry of the orbits of all observed satellites is known precisely. Obviously, repeated observations improve the accuracy of that point. This method allows one to locate a position without reference to any other point, the only disadvantage being that it takes a long time to get the required accuracy.

The translocation method requires simultaneous data from separate stations to determine the position of one station relative to the other. The main advantage of this method is that one can locate a point accurately with only a few passes of the *common* satellite (i.e., common to both the reference station and the translocated locations).

PHOTOGRAMMETRIC ENGINEERING & REMOTE SENSING,
Vol. 57, No. 9, September 1991, pp. 1217–1220.

0099-1112/91/5709–1217$03.00/0

TABLE 1. PANCHROMATIC SPOT IMAGES USED TO CONSTRUCT THE FINAL MOSAIC OF BUTON ISLAND.

No.	Path (K)	Row (J)	Date	Time (GMT)	Incidence	Azimuth (Sun)	Elevation (Sun)
A1	317	359	01/20/89	02:01:44	R 25.8	121.0	57.6
A2	317	359	11/29/88	02:01:46	R 25.4	128.5	61.6
A3	317	359	03/28/89	02:12:55	R 02.6	74.7	64.0
B1	317	360	01/20/89	02:01:53	R 25.8	120.5	57.8
B2	317	360	12/14/88	02:13:35	R 02.3	132.3	61.9
B3	317	360	06/20/88	02:16:38	L 06.0	37.5	53.6
C1	317	361	01/14/89	02:17:32	L 06.3	125.4	61.2
C2	317	361	06/20/88	02:16:47	L 06.0	37.1	53.2

Even on SPOT images acquired after the Doppler survey was completed, most Doppler points were difficult to recognize. Some points were marked by crosses of yellow-painted logs, each cross being roughly 20 metres across. Even in clearings, these crosses could not be seen on SPOT imagery. Some of the Doppler points were photographed from the air during September 1988. This proved essential to recognizing the Doppler points on the SPOT imagery, even though some of the Doppler points photographed from the air still could not be located on the SPOT imagery. This problem emphasizes the importance of referencing Doppler points to ground features that can be recognized without ambiguity on the SPOT imagery. This could be accomplished best if field Doppler parties had the SPOT imagery beforehand and sited their points with reference to ground landmarks that are prominent on the SPOT imagery. Such a procedure would also keep Doppler points from being unusable because they had been taken at sites that were obscured by clouds.

PROCESSING

The basic processing can be divided into two steps. The first step was to geometrically correct all the images. The second step was to combine these images to minimize cloud cover. Both of these steps are explained in some detail here.

CLOUD REMOVAL

Figure 1 shows the final mosaic of Buton, along with the two scenes that were processed pixel by pixel to generate the nearly cloud free northern portion of the mosaic.

The method used to remove clouds on a pixel-by-pixel basis is more complex than the method used by Zhirong and McDonnell (1986) to remove clouds from Heat Capacity Mapping Mission (HCMM) imagery of New Zealand. They used thresholds in both thermal infrared and visible near-infrared bands to recognize and remove cloudy pixels. It is harder to remove clouds from SPOT imagery than from HCMM because "land" and "cloud" pixels are not as distinct on SPOT imagery. Panchromatic SPOT data have only one band (0.51 to 0.73 μm), so clouds cannot be recognized by being colder than land. The higher resolution of SPOT (10 m versus 500 to 600 m) means that registration must be much more precise and that cloud shadows must be removed as well as clouds. Removing shadows proved to be a much harder task than removing clouds. Following is a detailed explanation of the method used.

Given two or more images of the same areas with complementary cloud cover, there are basically two ways to combine them. One method is to cut out the clouded areas from each image, then overlay one over the other. This method is fairly straightforward but, unless the images are similar in radiometric character, the seam lines are fairly visible. It is often necessary to match histograms of the distribution of brightness values in the two original images before mosaicking them together.

Another method is to compare two images of the same area on a pixel-by-pixel basis and then decide whether that pixel on each image represents cloud (bright), cloud's shadow (dark), or sunlit ground (intermediate). Then each cloudy or shadowed pixel is discarded if the corresponding pixel on the complementary image shows unobscured ground. This method requires very precise registration of the images and similar radiometric character to produce acceptable results.

Ideally, a selection algorithm should pick only those pixels which show sunlit ground and discard pixels that show clouds or their shadows. Our algorithm assigns pixels into these three categories by using threshold values of brightness at the upper and lower limits of the brightness of sunlit ground ("real data"). However, in reality there is an ambiguity between these cases because all three cases have a distribution of pixel values which overlap each other. For examples, the lowest value of a cloud pixel may be lower than the brightest real data pixel. In that case, depending on the threshold, the data pixel may be mistakenly chosen as the cloud value. Similarly, the highest value of a shadow pixel may be higher than the lowest data pixel's value, in which case the data pixel may be chosen as the shadow value and discarded. Furthermore, on the edges of all clouds and shadows, the pixel brightness value will record only the average brightness, which may be interpreted as real data. Following are some of algorithms which were tried for this exercise.

Algorithm 1.

```
Do for each corresponding pixel
  Choose the lower of two pixel values
End Do
```

The above algorithm removes the clouds, assuming that all data values are lower than the cloud values. This simple algorithm works extremely well in absence of any shadows. When there is a shadow, then this algorithm chooses the shadow value rather than the data value.

Algorithm 2.

```
Set the lower limit (ll) on the data values
Do for each corresponding pixel
  Choose the lower of two pixel values (say, ld1 < ld2)
  Compare ld and ll
  If ld1 > ll
    Choose ld1 for data value
  Else
    Choose ld2
  End If
End Do
```

This algorithm avoids choosing the shadow value by comparing it with a threshold. The selection of this threshold is obviously very important. One can choose a value based on the histograms of various parts of the image. A threshold which is higher than the lowest data value will choose shadows as the final value. It is also possible that the lowest data value is lower than the pixel value in shadow due to noise in the image, which would create an ambiguity in the selection process. This algorithm does not take into account the situation where the data value is comparable to the light cloud values. Thus it may actually choose the cloud value over real data in some instances.

Algorithm 3.

```
Set the lower limit (ll) on the data values of both images
Set the higher limit (hh) on the data values of both images
(The above limits may also be set for each image separately)
Do for each corresponding pixel
  Choose the lower of two pixel values (say, ld1 < ld2)
  Compare ld1 and ll1
```

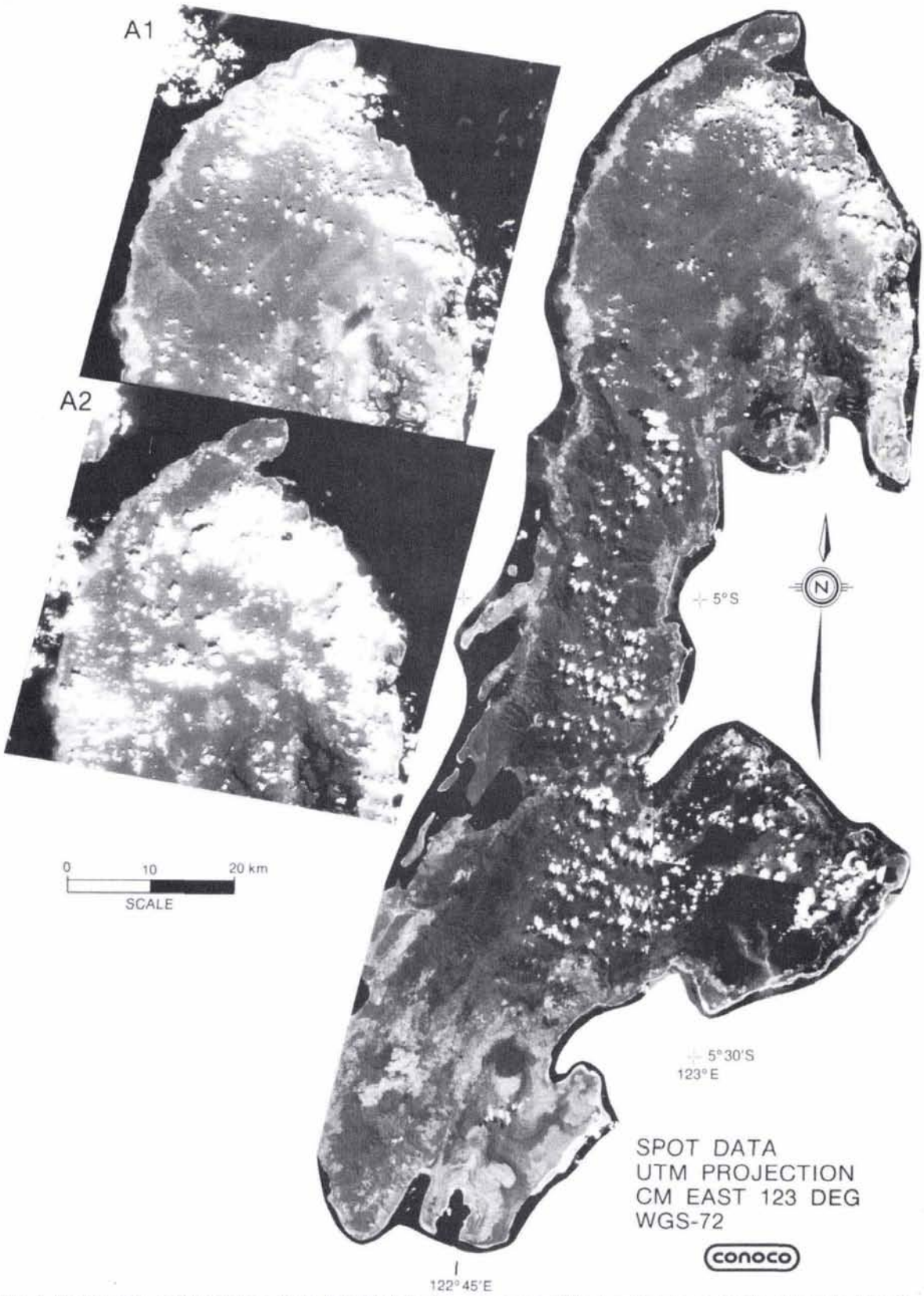

FIG. 1. Final mosaic of Buton Island. Refer to Table 1 for the scenes used. The two partial scenes (A1, A2) to the left of the mosaic were processed pixel by pixel to remove clouds in north Buton.

```
If Id1 > Il1
   Choose Id1 for data value
Else
   Choose Id2
```

```
  End If
  The value chosen so far is Id
  If Id < hh
    Choose Id for final pixel
  Else
    flag this as a cloud pixel in both images
End Do
```

This algorithm is quite similar to Algorithm 2 with the additional check for the cloud pixels.

Geometric Correction

Figure 2 illustrates the concept of transforming a distorted image grid to a regular image grid. The transformation is done through control points. Control points are simply pairs of x, y (or line, sample) coordinates of the same location on the distorted and corrected images, respectively. Given enough control points (generally more than four), one can define a pair of functions to predict the old location of a given new location as follows:

$$O_l = F(N_l, N_s)$$
$$O_s = F(N_l, N_s)$$

where N_l = new line, O_l = old line, N_s = new sample, and O_s = old sample.

There are many functions that can satisfy the above criteria. The VICAR image processing program has several choices of functions to choose from. Some of them are listed below:

Function Example 1.

$$O_l = J + IN_l + HN_s + GN_l^2 + FN_s^2 + EN_sN_l$$

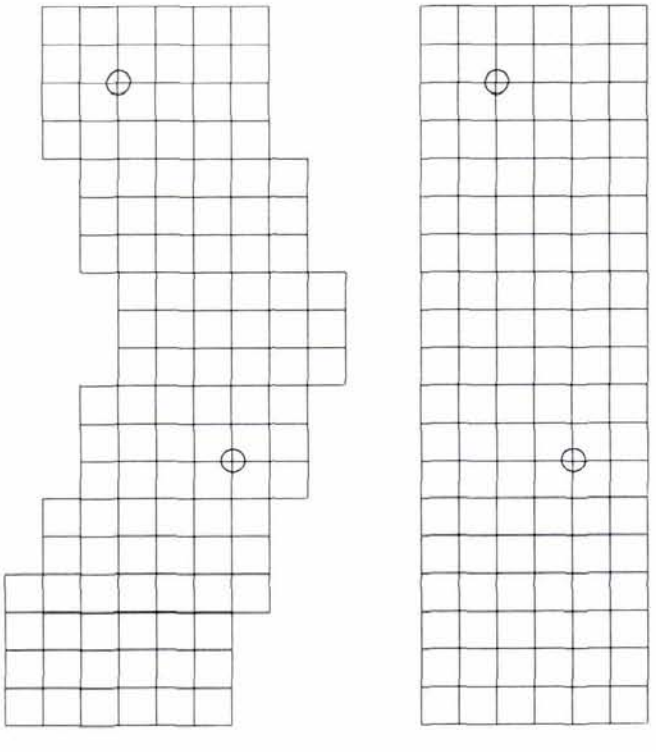

Before Correction *After Correction*

FIG. 2. Correction (rubber sheeting) of images. This figure shows the images before correction (left) and after correction (right). The circles represent the control points.

$$O_s = J + IN_l + HN_s + GN_l^2 + FN_s^2 + EN_sN_l$$

Function Example 2.

$$O_l = J + IN_l + HN_s + GN_l^2 + FN_s^2 + EN_sN_l + DN_lN_s^2 + CN_sN_l^2 + BN_l^3 + AN_s^3$$

$$O_s = J + IN_l + HN_s + GN_l^2 + FN_s^2 + EN_sN_l + DN_lN_s^2 + CN_sN_l^2 + BN_l^3 + AN_s^3$$

Function Example 3.

$$O_l = AN_l + BN_s + D$$
$$O_s = EN_l + FN_s + H$$

Function Example 4.

$$O_l = (AN_s - BN_l)mag + CN_s$$
$$O_s = (BN_s + AN_l)mag + CN_l$$

where *mag* is the magnification factor.

In all of the above examples letters *A, B, C, D, E, F, G, H, I, J* represent the regression constants. It is important to note that these example functions only predict the old location as a function of the new location; they do not indicate anything about the pixel value for that particular location. The selection of pixel value at the new location can be as simple as choosing the nearest value (nearest neighbor) or as complicated as a weighted average of several surrounding pixels.

SHORELINES

The new shoreline is based on the boundary between bright shoreline features (beach and coral reef) and dark deeper water offshore. This boundary extends beyond the low-tide shoreline in places where submerged deposits are bright enough to be seen on SPOT through the water column. This problem is particularly evident on reefs and in estuaries. The shoreline on existing maps appears to be based more closely on the low-tide shoreline, so islands and peninsulas may appear narrower and steep shorelines more embayed on the old shoreline than on the updated one. The extreme case of this effect is along the shore of northeast Buton, where islands appear off the updated shoreline that were absent off the old shoreline.

Systematic discrepancies between the old and updated shorelines are most evident in eastern and southern Buton, where they are as large as two kilometres — much larger than any tidal or tectonic effect along a coast that drops abruptly into deep water. The discrepancies are smallest on the north coast, where they are not discernible at the 1:250,000 scale of this map. Discrepancies elsewhere on the island are mostly in the form of discrete shifts in shoreline position without much change in shape. The discrepancies in south Buton are mostly a westward shift between the old and new shorelines. The discrepancies in east Buton are mostly a southward shift between the old and new shorelines.

ACKNOWLEDGMENTS

The authors would like to express their appreciation for the encouragement they received from Peter Gore (former Chief Geologist, Conoco Indonesia). In addition John Davidson and John Hughes (Conoco Indonesia) provided additional information which proved essential in ascertaining the final accuracy of the mosaic.

REFERENCE

Zhirong, Li, and M. J. McDonnell, 1986. Using dual thresholds for cloud and mosaicking. *International Journal of Remote Sensing*, 7(10):1349–1358.